

# *Wet Bulb Globe Temperature: indicating extreme heat risk on a global grid*

Article

Published Version

Creative Commons: Attribution 4.0 (CC-BY)

open access

Brimicombe, C., Lo, C. H. B., Pappenberger, F., Di Napoli, C., Maciel, P., Quintino, T., Cornforth, R. ORCID: <https://orcid.org/0000-0003-4379-9556> and Cloke, H. L. ORCID: <https://orcid.org/0000-0002-1472-868X> (2023) Wet Bulb Globe Temperature: indicating extreme heat risk on a global grid. *GeoHealth*, 7 (2). e2022GH000701. ISSN 2471-1403 doi: <https://doi.org/10.1029/2022GH000701> Available at <https://centaur.reading.ac.uk/110531/>

It is advisable to refer to the publisher's version if you intend to cite from the work. See [Guidance on citing](#).

To link to this article DOI: <http://dx.doi.org/10.1029/2022GH000701>

Publisher: Wiley

All outputs in CentAUR are protected by Intellectual Property Rights law, including copyright law. Copyright and IPR is retained by the creators or other copyright holders. Terms and conditions for use of this material are defined in the [End User Agreement](#).

[www.reading.ac.uk/centaur](http://www.reading.ac.uk/centaur)

**CentAUR**

Central Archive at the University of Reading

Reading's research outputs online

## Wet Bulb Globe Temperature: Indicating Extreme Heat Risk on a Global Grid



### Key Points:

- We create an accurate method for calculating Wet Bulb Globe Temperature (WBGT) using Mean Radiant Temperature termed WBGT<sub>Brimicombe</sub>
- It is found that WBGT<sub>amsc87</sub> also known as WBGTsimple is not an accurate approximation of WBGT
- WBGT<sub>Brimicombe</sub> can assist with robust heat stress standards across sectors including in public and occupational health

### Correspondence to:

C. Brimicombe,  
c.r.brimicombe@pgr.reading.ac.uk

### Citation:

Brimicombe, C., Lo, C. H. B., Pappenberger, F., Di Napoli, C., Maciel, P., Quintino, T., et al. (2023). Wet Bulb Globe Temperature: Indicating extreme heat risk on a global grid. *GeoHealth*, 7, e2022GH000701. <https://doi.org/10.1029/2022GH000701>

Received 8 AUG 2022

Accepted 7 FEB 2023

### Author Contributions:

**Conceptualization:** Chloe Brimicombe, Florian Pappenberger

**Formal analysis:** Chloe Brimicombe

**Investigation:** Chloe Brimicombe, Tiago Quintino

**Methodology:** Chloe Brimicombe, Chun Hay Brian Lo, Florian Pappenberger, Claudia Di Napoli, Pedro Maciel

**Resources:** Chloe Brimicombe, Claudia Di Napoli, Tiago Quintino

**Software:** Chloe Brimicombe, Chun Hay Brian Lo, Pedro Maciel, Tiago Quintino

**Supervision:** Florian Pappenberger, Hannah L. Cloke

**Visualization:** Chloe Brimicombe

**Writing – original draft:** Chloe Brimicombe

Chloe Brimicombe<sup>1,2,3</sup> , Chun Hay Brian Lo<sup>4</sup>, Florian Pappenberger<sup>2</sup> , Claudia Di Napoli<sup>1,5</sup> , Pedro Maciel<sup>2</sup> , Tiago Quintino<sup>2</sup>, Rosalind Cornforth<sup>3</sup>, and Hannah L. Cloke<sup>1,4,6,7</sup> 

<sup>1</sup>Department of Geography and Environmental Science, University of Reading, Reading, UK, <sup>2</sup>European Centre for Medium-Range Weather Forecasts (ECMWF), Reading, UK, <sup>3</sup>Walker Institute, University of Reading, Reading, UK, <sup>4</sup>Department of Meteorology, University of Reading, Reading, UK, <sup>5</sup>School of Agriculture, Policy and Development, University of Reading, Reading, UK, <sup>6</sup>Department of Earth Sciences, Uppsala University, Uppsala, Sweden, <sup>7</sup>Centre of Natural Hazards and Disaster Science, CNDS, Uppsala, Sweden

**Abstract** The Wet Bulb Globe Temperature (WBGT) is an international standard heat index used by the health, industrial, sports, and climate sectors to assess thermal comfort during heat extremes. Observations of its components, the globe and the wet bulb temperature (WBT), are however sparse. Therefore WBGT is difficult to derive, making it common to rely on approximations, such as the ones developed by Liljegren et al. (2008, <https://doi.org/10.1080/15459620802310770>, WBGT<sub>Liljegren</sub>) and by the American College of Sports Medicine (WBGT<sub>ACSM87</sub>). In this study, a global data set is created by implementing an updated WBGT method using ECMWF ERA5 gridded meteorological variables and is evaluated against existing WBGT methods. The new method, WBGT<sub>Brimicombe</sub>, uses globe temperature calculated using mean radiant temperature and is found to be accurate in comparison to WBGT<sub>Liljegren</sub> across three heatwave case studies. In addition, it is found that WBGT<sub>ACSM87</sub> is not an adequate approximation of WBGT. Our new method is a candidate for a global forecasting early warning system.

**Plain Language Summary** The Wet Bulb Globe Temperature (WBGT) is an international standard for how we measure the effect of heat on the human body. It is used across sectors in health, industry, sports, and climate to calculate how we feel and how our body responds during heat extremes. Its calculation has historically relied on globe thermometer and wet bulb temperature observations, which are however not widely available. This has made WBGT difficult to calculate and meant approximations have been created. Here we formulate a new WBGT method that can be used with global gridded data that are freely available and we compare it against other methods in common use. We find that our method is accurate when compared to the existing gold standard WBGT method.

## 1. Introduction

The Wet Bulb Globe Temperature (WBGT) is an International Standards Organisation (ISO) approved metric of heat stress in humans (Int Org Standard, 2017). Heat stress is caused by the build-up of body heat either as a result of exertion and/or exposure to the external environment (air temperature humidity, solar radiation, wind speed etc.) (D'Ambrosio Alfano et al., 2014; Ioannou et al., 2022; Jacklitsch et al., 2016; McGregor & Vanos, 2018; Parsons, 2006). WBGT was originally developed in the 1950s as part of a campaign to lower the risk of heat disorders during the training of US Army and Marine troops (Minard, 1961).

The WBGT has many applications and is used widely in many research areas such as the occupational and public health sectors. In addition, it is used in the sports and exercise field, industrial hygiene and in climate change research and is one of the most popular heat stress indices (Heo et al., 2019; Kjellstrom et al., 2009; Lemke & Kjellstrom, 2012; Lucas et al., 2014; Racinais et al., 2015).

The WBGT (°C) is defined by three environmental variables via the following equation (Minard, 1961):

$$\text{WBGT} = 0.7T_w + 0.2T_g + 0.1T_a \quad (1)$$

where  $T_a$  is 2 m air temperature (i.e., dry bulb temperature, in °C),  $T_g$  is globe thermometer temperature (°C), and  $T_w$  is natural wet bulb thermometer temperature (°C).

**Writing – review & editing:** Chun Hay Brian Lo, Florian Pappenberger, Claudia Di Napoli, Tiago Quintino, Rosalind Cornforth, Hannah L. Cloke

Whereas 2 m air temperature is easily measurable, observations of globe thermometer and wet bulb thermometer temperatures are often sparse (Budd, 2008; D’Ambrosio Alfano et al., 2014). Consequently, it has been historically challenging to calculate WBGT from Equation 1 and it is instead common to rely on approximations. These include the approximation from the American College of Sports Medicine (termed WBGT<sub>ACSM87</sub>), which is a linear model of the WBGT (American college of sports medicine, 1987), and the approximation by Liljegren and colleagues (termed WBGT<sub>Liljegren</sub>), which is a more complex approximation based on the fundamentals of heat transfer (Liljegren et al., 2008).

In this study, we compare a new approach to approximate WBGT (termed WBGT<sub>Brimicombe</sub>) with WBGT<sub>ACSM87</sub> and WBGT<sub>Liljegren</sub>. Our approach is novel in calculating WBGT from gridded data using the variable of mean radiant temperature and is designed for operational forecasting systems. Comparisons are performed globally by using the ERA5 hourly global gridded reanalysis from the European Centre for Medium-Range Weather Forecasts (ECMWF), Observation data from the World Radiation Monitoring Center–Baseline Surface Radiation Network (Driemel et al., 2018) and are here discussed within the context of three heatwave case studies (India and Pakistan in July 2003, the Western Sahel in March 2013 and Australia in December 2019).

## 2. Method

### 2.1. Brimicombe WBGT Approximation (WBGT<sub>Brimicombe</sub>)

This new approach to approximate WBGT has been developed for numerical weather prediction post-processing as it takes an optimized approach to the calculation of WBGT by removing the need for iterative loops. We calculate globe temperature using an adapted version of the original Bedford and Warner equation, making use of mean radiant temperature, a measurement of incidence of radiation on a body which is appropriate for indoor or outdoor use depending on given inputs (Bedford & Warner, 1934; De Dear, 1987; Guo et al., 2018; Thorsson et al., 2007; Vanos et al., 2021).

Here Equation 2 is used to solve for globe temperature as the subject because the ERA5 reanalysis data contains the variables of 2 m air temperature ( $T_a$ ), 10-m wind speed ( $v_a$ ), and mean radiant temperature ( $T_{MRT}$ ). All temperatures are in Kelvin; 10-m wind speed was found to be within  $\pm 1^\circ\text{C}$  of an approximated 2 m wind speed which used the method found in Spangler et al. (2022) and therefore is used (not shown). The code to compute this is available as part of thermofeel: <https://doi.org/10.21957/mp6v-fd16> (Brimicombe et al., 2021; Brimicombe, Di Napole et al., 2022)

$$T_{MRT} = \sqrt[4]{T_g^4 + \frac{h_{cg}}{\epsilon \times D^{0.4}} \times (T_g - T_a)} \quad (2)$$

In Equation 2,  $h_{cg}$  is the mean convection coefficient and is calculated using Equation 3. This is an additional correction from the original method and reduces the impact weighting of high wind speeds on the outputted globe temperature (De Dear, 1987; Guo et al., 2018).

$$h_{cg} = 1.1 \times 10^8 \times v_a^{0.6} \quad (3)$$

To calculate the wet bulb temperature (WBT), a theoretical method by Stull (2011) is used and is shown in Equation 4, where  $T_a$  is 2 m air temperature in  $^\circ\text{C}$  and RH is relative humidity in percent. This method is valid between  $-20^\circ\text{C}$  and  $50^\circ\text{C}$  and between 5% and 99% humidity, which are the ranges the method is optimized for and with which it has been used in previous studies (Freychet et al., 2020; Heo et al., 2019; Raymond et al., 2017). In addition, this method provided a test case, an expected value for a given set of inputs, which allowed validation of the calculated value (Stull, 2011).

$$\begin{aligned} T_w = & T_a \tan^{-1}(0.151977(\text{RH} + 8.313659)^{1/2}) \\ & + \tan^{-1}(T_a + \text{RH}) \\ & - \tan^{-1}(\text{RH} - 1.676331) + 0.00391838(\text{RH})^{3/2} \\ & \times \tan^{-1}(0.023101 \times \text{RH}) - 4.686035 \end{aligned} \quad (4)$$

Once calculated, the globe temperature and WBT along with 2 m air temperature are used in Equation 1 to provide the WBGT<sub>Brimicombe</sub> approximation.

## 2.2. Liljegren WBGT Approximation ( $WBGT_{Liljegren}$ )

$WBGT_{Liljegren}$  can be considered a existing “gold standard” benchmark WBGT value as it is widely considered the most accurate WBGT approximation available (Kjellstrom et al., 2009; Kong & Huber, 2021; Liljegren et al., 2008). To obtain  $WBGT_{Liljegren}$ , WBT is calculated as per Equation 5 and globe temperature is calculated as per Equation 6 which are then used in Equation 1. Specifically, WBT is calculated as

$$T_w = T_a - Nu \times Sh \times \left(\frac{Pr}{Sc}\right)^a \left(\frac{e_w - e_a}{P - e_w}\right) + \frac{\Delta F_{net}}{A_h} \quad (5)$$

where Nu is the Nusselt number, Sh is the Sherwood Number, Pr is the Prandtl number, and Sc is the Schmidt number and  $\left(\frac{e_w - e_a}{P - e_w}\right)$  is the change in saturation water vapor transfer between the hygrometer wick and its surroundings.  $\frac{\Delta F_{net}}{A_h}$  is the net radiative heat flux divided by the convective heat transfer coefficient. Full details can be seen in (Liljegren et al., 2008). Globe temperature is calculated as

$$T_g^4 = \frac{1}{2}(1 + \epsilon_a)T_a^4 - \frac{h}{\epsilon_g \sigma} (T_g - T_a) + \frac{ssrd}{2\epsilon_g \sigma} (1 - \alpha_g) \left[1 + \left(\frac{1}{2 \cos \theta}\right) dsrp + \alpha_{sfc}\right] \quad (6)$$

where the  $\frac{h}{\epsilon_g \sigma} (T_g - T_a)$  and  $\frac{S}{2\epsilon_g \sigma} (1 - \alpha_g)$  terms denote the energy gain from diffuse downwards and direct downward solar radiation respectively. dsrp is the projected area and  $\alpha_{sfc}$  is the reflected solar radiation and ssrd is downward solar radiation. Full details can be seen in Liljegren et al. (2008). Here data for  $WBGT_{Liljegren}$  is provided by Kong and Huber (2021), instead of calculation using the HEAT-SHIELD methodology, because the method presented by Kong and Huber appears to be more robust and closer to the original methodology (Casanueva, 2017).

## 2.3. American College of Sports Medicine WBGT Approximation ( $WBGT_{ACSM87}$ )

The  $WBGT_{ACSM87}$  (American college of sports medicine, 1987) was also calculated (Equation 7) as it continues to appear widely in literature, despite it being known to have large bias (Chen et al., 2019; Grundstein & Cooper, 2018; Kong & Huber, 2021).  $WBGT_{ACSM87}$  is calculated from 2 m air temperature and saturation water vapor pressure (e) as:

$$WBGT_{ACSM87} = 0.567 \times T_a + 0.393 \times e + 3.94 \quad (7)$$

## 2.4. Methodological Difference Between $WBGT_{Brimicombe}$ and $WBGT_{Liljegren}$

Several methodological differences between our new WBGT approximation and the existing “gold standard” WBGT approximation are present (Brimicombe, Di Napoli et al., 2022; Liljegren et al., 2008).

One key variable that is necessary in the calculation of  $T_g$  (both in Equations 2 and 6) is the cosine of the solar zenith angle. In previous studies it is found that radiation in the Liljegren  $T_g$  methodology has inaccuracies at sunrise and sunset due to the method used to calculate this variable (Kong & Huber, 2022; Lemke & Kjellstrom, 2012). These inaccuracies are known to become greater in a numerical weather prediction service time step (a period of several hours) (Brimicombe, Quintino, et al., 2022; Hogan & Hirahara, 2016). For the Brimicombe  $T_g$  methodology this does not occur because a specially designed cosine of the solar zenith angle is implemented (Brimicombe, Di Napoli et al., 2022; Brimicombe, Quintino, et al., 2022).

Another difference is in the number of radiation input variables used to calculate  $T_g$  in the Liljegren methodology. In this only 2 radiation components are used (Liljegren et al., 2008) in comparison to the 5 that calculate  $T_{MRT}$  (please refer to: Di Napoli et al., 2020) which goes on to calculate the Brimicombe  $T_g$ . Equation 2, which expresses mean radiant temperature  $T_{MRT}$  as a function of  $T_g$  and  $T_a$ , is comparable to the heat balance expressed in Bedford and Warner (1934), therefore relating mean radiant temperature to the temperature of surrounding surfaces. Similarly, Equation 2 can also be rearranged in order of  $T_g^4$ , where many comparable terms to Equation 6 are identifiable.

In the Liljegren  $T_w$  methodology a psychrometric WBT is calculated using fundamentals of mass transfer. In addition a key input of saturation water vapor pressure is calculated differently over ice and water (and the land

**Table 1**  
*Heat Stress Thresholds for Wet Bulb Globe Temperature and Recommended Labor Legal Definitions of Workloads for an Average Period of Work*

| WBGT (°C) | Recommended maximum workload | Approximated work/rest cycles (minutes) | Category |
|-----------|------------------------------|---|----------|
| >33       | Resting                      | Rest                                    | 5        |
| 30–33     | Light                        | 15/45                                   | 4        |
| 28–30     | Moderate                     | 30/30                                   | 3        |
| 25–28     | Heavy                        | 30/15                                   | 2        |
| 23–25     | Very heavy                   | 45/15                                   | 1        |
| <23       | No recommendations           | No recommendations                      | 0        |

Note. Adapted from Jacklitsch et al. (2016).

surface) as in Hardy (1998). In comparison, in the Brimicombe  $T_w$  methodology an empirical theoretical WBT is calculated (Stull, 2011). As previously mentioned, this computationally removes the need for iterative loops, which are onerous to run for a gridded data set. In addition, the saturation water vapor pressure method is only for over water (and the land surface) in contrast to being over either water or ice, given that WBGT is a human heat stress index. How these methodological differences introduce errors will be explored within this study.

### 2.5. WBGT Approximation Comparisons

To compare the WBGT approximations, this study uses variables available as part of the ERA5 and ERA5-HEAT gridded reanalysis data sets produced by ECMWF on a  $0.25^\circ \times 0.25^\circ$  grid at an hourly time step (Di Napoli et al., 2021; Hersbach et al., 2020). ERA5 was chosen for this study as a state-of-the-art gridded reanalysis data set; it is an ideal data set to test out a

new gridded based methodology and has the added benefit of outputting the mean radiant temperature variable (the incidence of radiation on the body). ERA5 and ERA5-HEAT variables of 2 m air temperature, 2 m dew point temperature, 10 m wind speed and mean radiant temperature are used in the relevant equations to calculate  $WBGT_{Brimicombe}$  and  $WBGT_{ACSM87}$ .  $WBGT_{Liljegen}$  is also calculated using ERA5 reanalysis data. There are known limitations of ERA5; these include inaccuracies at higher elevations (Brunamonti et al., 2019; Senyuzni et al., 2020).

The approximations are calculated and compared for three past heatwaves on dates where heat stress is known to have occurred. One affected India and Pakistan in July 2003, another the Western Sahel in March 2013 and another Australia in December 2019 (CRED, 2020). In addition, this study also considers the full global gridded data sets of WBGT values including those below a heat stress threshold.

The gridded ERA5 reanalysis output for  $WBGT_{Brimicombe}$  is compared to the observed  $WBGT_{Brimicombe}$  calculated using data from the Tateno TAT ( $36.1^\circ N$ ,  $140^\circ E$ ) and Nya Långnäs NYA ( $78.9^\circ N$ ,  $11^\circ E$ ) stations from the World Radiation Monitoring Center–Baseline Surface Radiation Network (WRMC–BSRN, Driemel et al., 2018) for Daily Maximum WBGT for July 2003 and March 2013. In addition, for March 2013 the Stull WBT method is compared to the Davies-Jones method (available at: <https://github.com/smartlxxx/WetBulb/blob/master/WetBulb.py>) (Davies-Jones, 2008; Stull, 2011). We are constrained by the available observation data.

The comparison between the three approximations uses the observed WBGT thresholds set out by the ISO (Jacklitsch et al., 2016; Table 1). According to ISO, which considers heat stress by reference to recommended lifting and hard labor workloads,  $33^\circ C$  is known as a critical health threshold for WBGT (Heo et al., 2019).

$WBGT_{ACSM87}$  and  $WBGT_{Brimicombe}$  are compared against the existing gold standard approximation of  $WBGT_{Liljegen}$  in two ways. The first is through evaluation of the spatial anomaly in WBGT values.  $WBGT_{Liljegen}$  is subtracted from the corresponding  $WBGT_{ACSM87}$  or  $WBGT_{Brimicombe}$  values. Second, is a correlation between  $WBGT_{Liljegen}$  and the other WBGT approximations is assessed together with the mean absolute error (MAE). In addition the sensitivity of the outputted  $WBGT_{Brimicombe}$  and  $WBGT_{Liljegen}$  approximations to key input variables is assessed.

## 3. Results

### 3.1. Gridded Outputs of WBGT for the Three Heatwaves

In July 2003, the highest values of  $WBGT_{Liljegen}$  are over  $33^\circ C$  for the border of northern India and Pakistan, which is indicative of extreme heat stress in category 5 (Figure 1, left column). This pattern is well matched by  $WBGT_{Brimicombe}$ . The lowest values for both of these WBGT approximations are over the Himalayas bordering the north-east of India, indicating no heat stress.  $WBGT_{ACSM87}$  has lower heat stress values and only reaches  $33^\circ C$ , category 4.

In March 2013, the highest values of  $WBGT_{Liljegen}$  are over  $33^\circ C$  and are indicative of extreme heat stress (category 5) for the north of Ghana and Nigeria (Figure 1, middle column). This pattern is broadly matched by



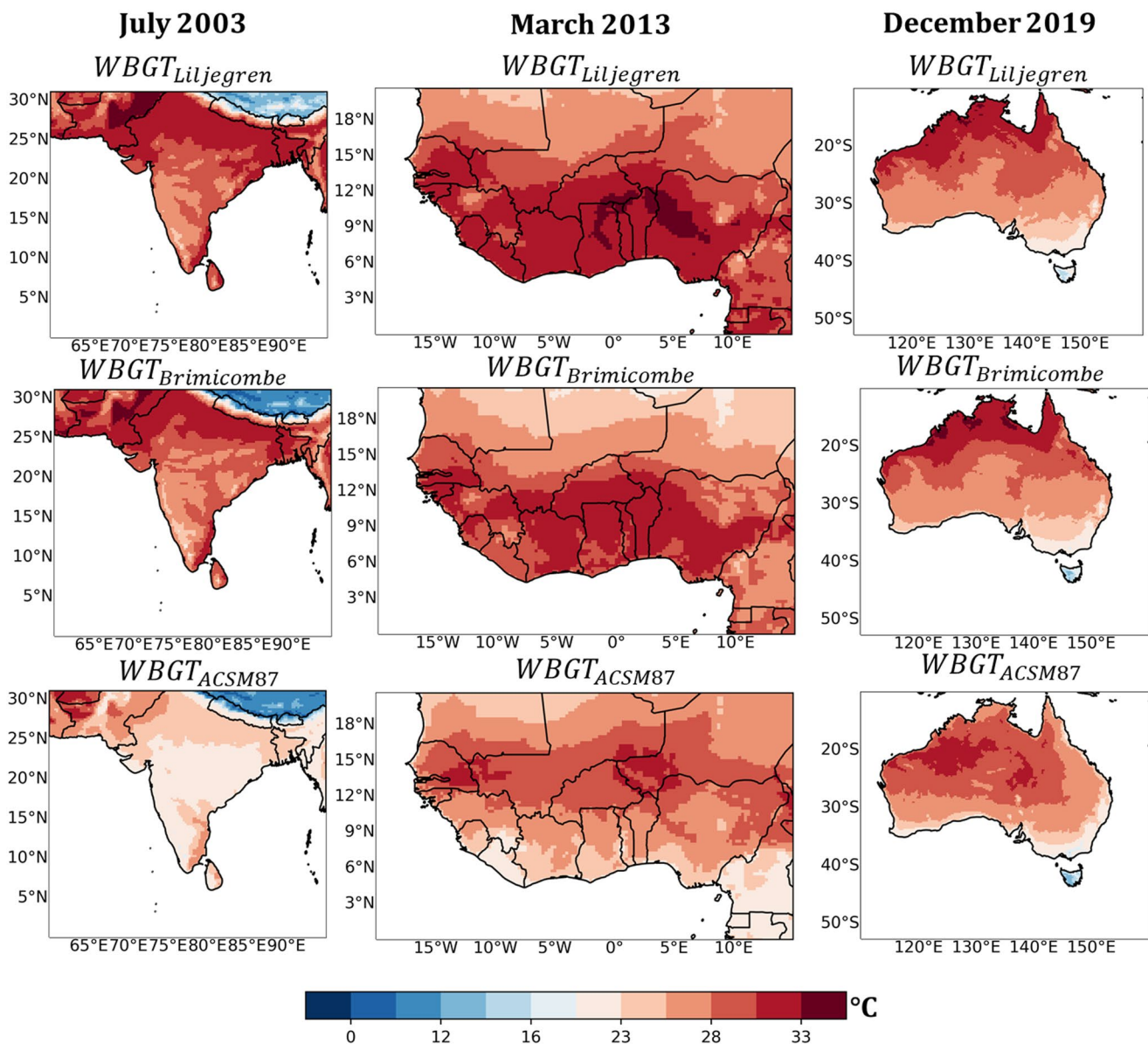


**Figure 1.** Heat stress calculated via  $WBGT_{Liljegren}$ ,  $WBGT_{Brimicombe}$  and  $WBGT_{ACSM87}$ . Monthly mean of daily maximum Wet Bulb Globe Temperature heat stress (left to right) for the heatwaves that affected India and Pakistan in July 2003, the Western Sahel in March 2013, and Australia in December 2019. Sea area has been masked.

$WBGT_{Brimicombe}$  although the extreme region of heat stress has slightly lower values. Similarly to the July 2003 heatwave,  $WBGT_{ACSM87}$  has much lower values than the other approximations and only reaches at the maximum up to 33°C (category 4) in one small area. The pattern of heat stress is not well captured and  $WBGT_{ACSM87}$  is consistently at least two heat stress categories lower than  $WBGT_{Liljegren}$  and  $WBGT_{Brimicombe}$  over the whole region.

For the heatwave of December 2019 in Australia, there are strikingly similar heat stress patterns for  $WBGT_{Liljegren}$  and  $WBGT_{Brimicombe}$  (Figure 1, right column).  $WBGT_{ACSM87}$  also performs better for this heatwave than for the July 2003 and March 2013 heatwaves and heat stress values are close to those of  $WBGT_{Liljegren}$ . However,  $WBGT_{ACSM87}$  again does not capture the same shape of the areas under heat stress.

These similarities and differences can also be seen clearly at the global scale for each heatwave (Figure 2).  $WBGT_{Liljegren}$  and  $WBGT_{Brimicombe}$  values are similar worldwide in each of the 3 months considered (Figure 2), particularly focusing on parts of North Africa, southern Asia and Australia. It is however noteworthy that  $WBGT_{Brimicombe}$  does not always capture the highest heat stress category indicated by  $WBGT_{Liljegren}$  in South

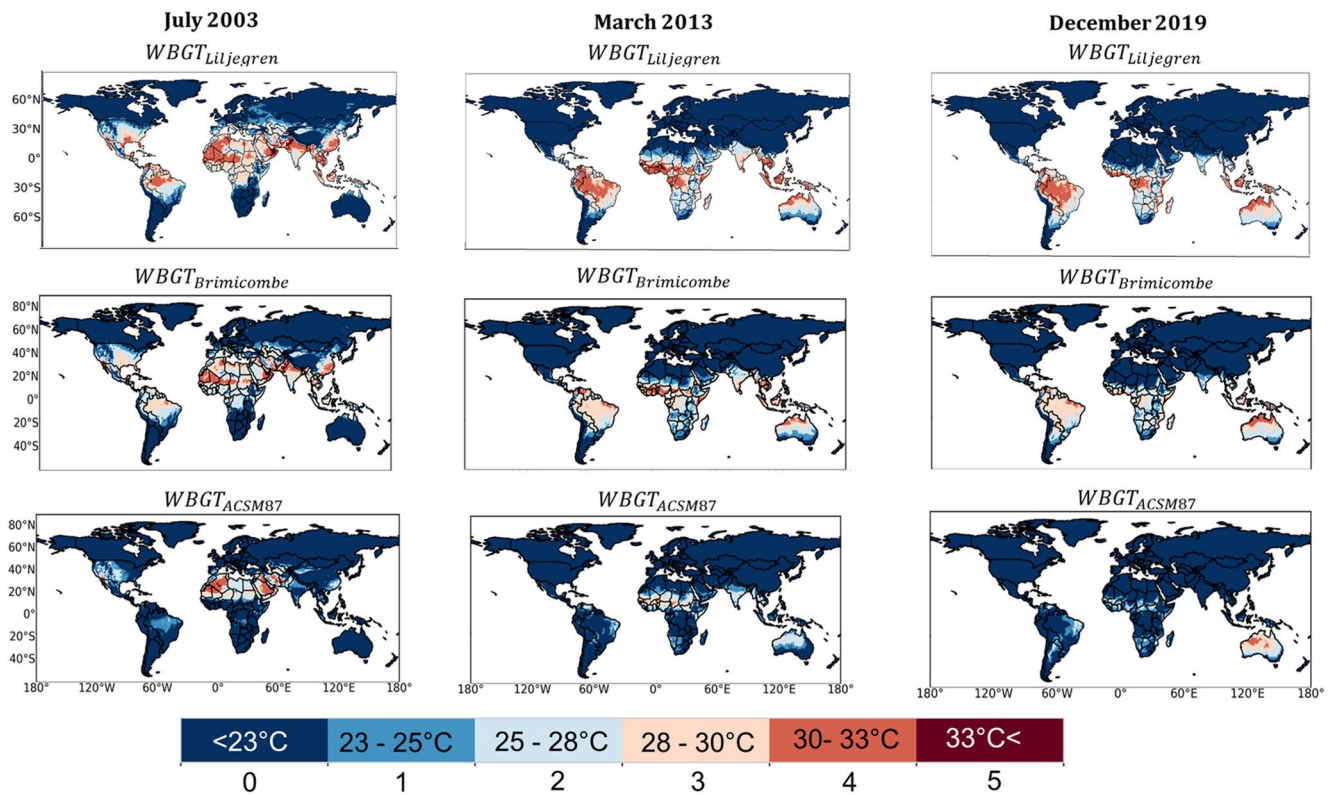


**Figure 2.** Categorical heat stress calculated via  $WBGT_{Brimicombe}$ ,  $WBGT_{ACSM87}$ , and  $WBGT_{Liljegren}$ . Monthly mean of daily maximum Wet Bulb Globe Temperature (WBGT) heat stress (left to right) for the heatwaves of July 2003, March 2013, and December 2019. Categories refer to the different levels of WBGT as indicated in Table 1. Sea area has been masked.

America (Figure 2).  $WBGT_{ACSM87}$  is very different from the other approximations on a global scale. It consistently has heat stress values that are too low, sometimes three heat stress categories lower, and only captures the heat stress in some parts of Australia.

### 3.2. WBGT Approximations Anomalies

Overall, the anomalies between  $WBGT_{Liljegren}$  and  $WBGT_{Brimicombe}$  are small, with negative anomalies indicating where  $WBGT_{Liljegren}$  has higher values than  $WBGT_{Brimicombe}$ , the term anomaly is used to denote deviations of WBGT approximations in comparison to the current gold standard  $WBGT_{Liljegren}$ . In July 2003,  $WBGT_{Liljegren}$  has higher values than  $WBGT_{Brimicombe}$  across most of the land surface (Figure 3, left column). In addition, anomalies can be seen to be no more or less than  $\pm 2^\circ\text{C}$ , except in Greenland which has anomalies of up to  $-4^\circ\text{C}$ . In comparison, March 2013 has a similar pattern where anomalies can be seen to not be more or less than  $\pm 2^\circ\text{C}$  between  $WBGT_{Liljegren}$  and  $WBGT_{Brimicombe}$  (Figure 3, middle column). However, for March 2013, more of the northern hemisphere has anomalies of  $-4^\circ\text{C}$ , for example, in Canada and Siberia colder regions. Fewer regions experience anomalies of  $-4^\circ\text{C}$  for December 2019, with this only present in the Himalaya into Tibet and the Canadian Rockies regions of higher elevation (Figure 3, right column). Overall across each of the three case studies, most of the land surface has anomalies of only  $\pm 2^\circ\text{C}$  between  $WBGT_{Liljegren}$  and  $WBGT_{Brimicombe}$ .

For  $WBGT_{Liljegren}$  in comparison to  $WBGT_{ACSM87}$  averaging across all years for the southern hemisphere,  $WBGT_{Liljegren}$  have values higher than  $WBGT_{ACSM87}$  by  $4^\circ\text{C}$ . In contrast, for the March 2013 and December 2019 heatwaves, the northern hemisphere has anomalies of  $+4^\circ\text{C}$ . Anomalies are less in the Sahara desert and Australia. For the July 2003 heatwave, anomalies match with those seen in the Southern hemisphere of  $-4^\circ\text{C}$ .

### 3.3. WBGT Approximations Correlations

Across both  $WBGT_{ACSM87}$  and  $WBGT_{Brimicombe}$  there is a strong linear correlation to  $WBGT_{Liljegren}$  (Figure 4).  $WBGT_{Brimicombe}$  has smaller MAE values across all three case studies than  $WBGT_{ACSM87}$ , with the smallest value



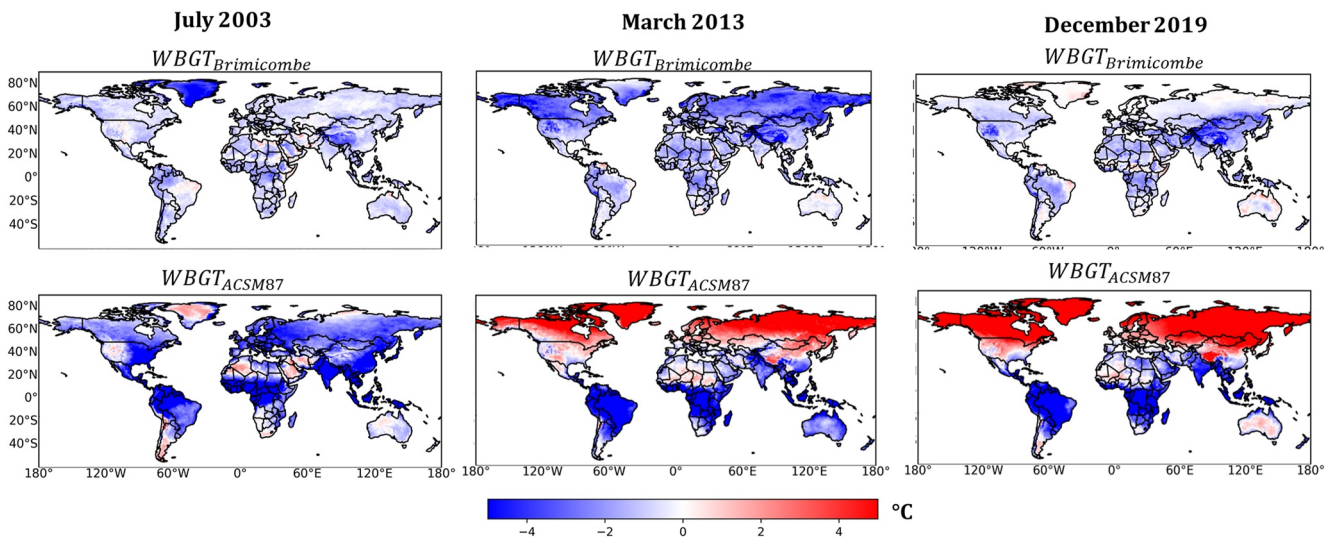


**Figure 3.** The monthly mean of the daily maxima anomalies of  $WBGT_{Brimicombe}$  and  $WBGT_{ACSM87}$  in comparison to  $WBGT_{Liljegen}$  for the three heatwaves considered by this study for July 2003, March 2013, and December 2019. Negative values are where  $WBGT_{Liljegen}$  has higher values than the other approximations.

being  $0.76^{\circ}\text{C}$ , being on average smaller for values about the heat stress threshold.  $WBGT_{ACSM87}$  MAE values are large and range between  $3.39^{\circ}\text{C}$  and  $5.51^{\circ}\text{C}$  across the three case studies but are significantly smaller above the heat stress threshold ranging from  $2.87^{\circ}\text{C}$  to  $3.11^{\circ}\text{C}$ .  $WBGT_{Brimicombe}$  heat stress values (above  $23^{\circ}\text{C}$ , category 1 onwards) have a stronger linear relationship than across the whole distribution. In comparison,  $WBGT_{ACSM87}$  has a bigger spread in the cluster of points than  $WBGT_{Brimicombe}$  over the whole distribution.

### 3.4. WBGT Approximation Differences

It has already been demonstrated that  $WBGT_{ACSM87}$  differs significantly from the other WBGT approximations presented. Therefore, here the sensitivity of only  $WBGT_{Liljegen}$  and  $WBGT_{Brimicombe}$  to key input variables is shown in more depth. Figure 5 demonstrates that broadly for both  $WBGT_{Liljegen}$  and  $WBGT_{Brimicombe}$  high solar radiation, temperature, humidity with low wind speeds lead to the highest WBGT values. In Figure 5 similarly to Figure 4 a bifurcation is seen for 2 m temperature (Figure 4) and somewhat for dew point temperature (Figure 4)

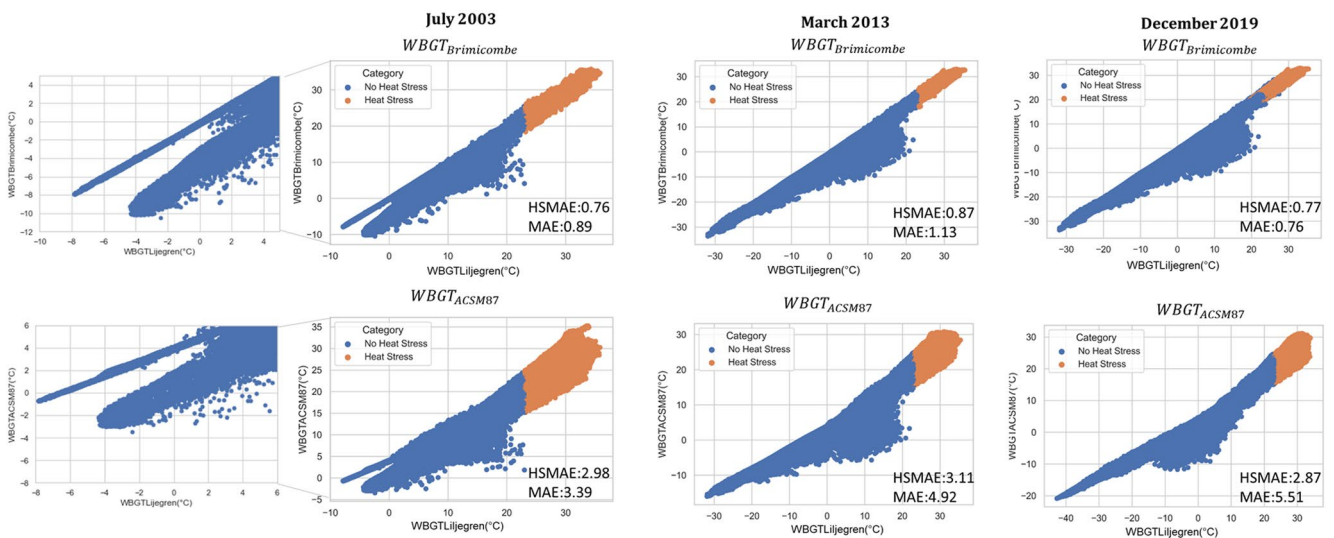


**Figure 4.** Global Grid Spatial Domain Correlation plots of  $WBGT_{Brimicombe}$  and  $WBGT_{ACSM87}$  in comparison to  $WBGT_{Liljegen}$  (orange indicated heat stress, i.e., Wet Bulb Globe Temperature values above  $23^{\circ}\text{C}$ ). The mean absolute error ( $^{\circ}\text{C}$ ) for all points and just the heat stress points is indicated in each plot for the three heatwaves considered by this study (July 2003, March 2013, and December 2019).

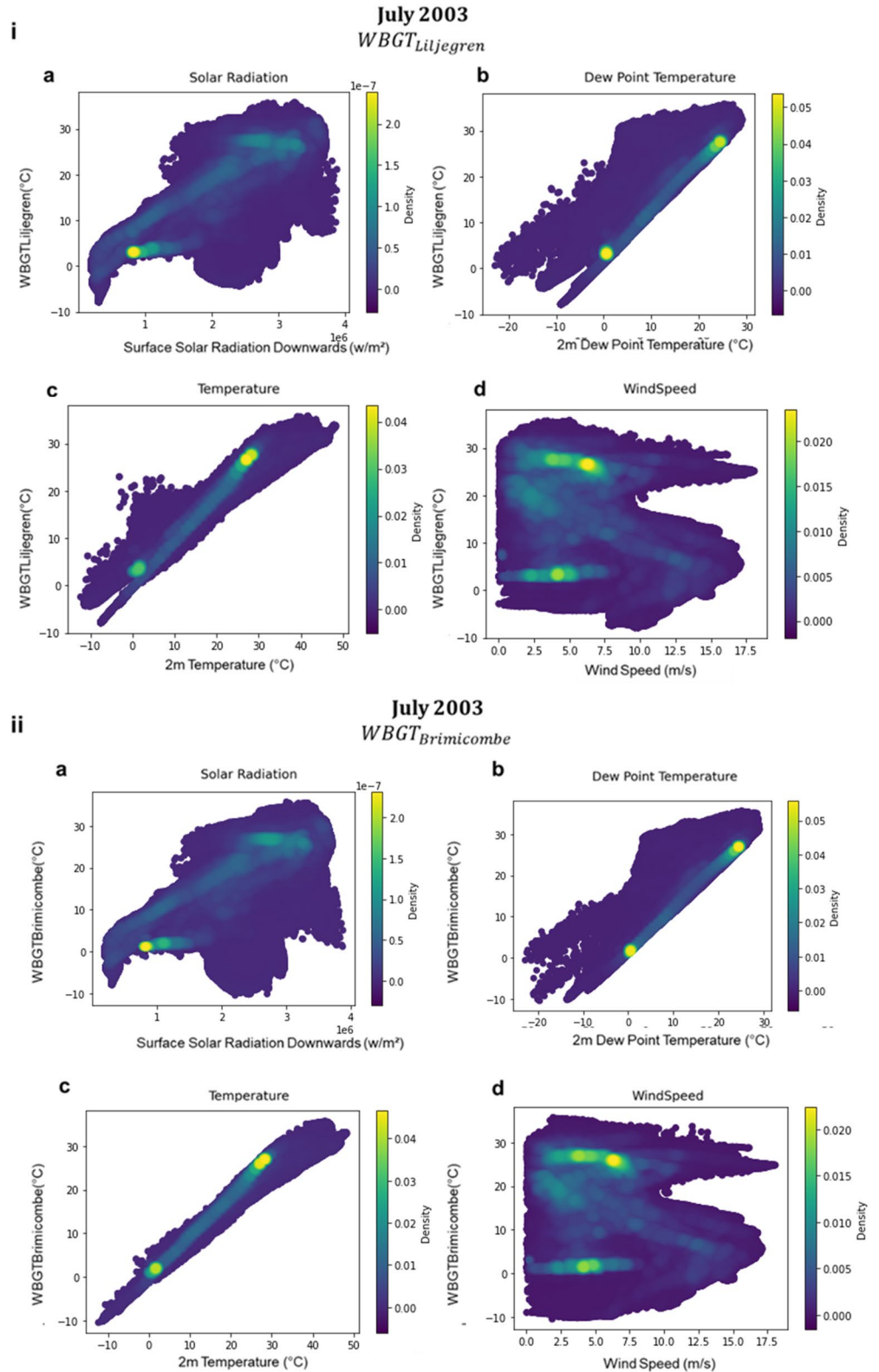


**Figure 5.** Global Grid Spatial Domain of the sensitivity of the output Wet Bulb Globe Temperature (WBGT) approximations with input variables for the July 2003 heatwave where (i) is  $WBGTL_{Liljegren}$  and (ii) is  $WBGTL_{Brimicombe}$  and where (a) is surface solar radiation downwards, (b) is 2 m dew point temperature, (c) is 2 m temperature, and (d) is 10 m wind speed. Input variables shown are those that are input to both WBGT approximations. Color shading denotes density of points. A similar relationship is observed for the other two heatwaves (not shown).

with the outputted  $WBGT_{Liljegen}$ . This confirms the trend is due to the  $WBGT_{Liljegen}$  Saturation Water Vapor pressure method (Figure 4). As suggested in Section 2.4 this discrepancy comes from the difference in the Tw methodology, specifically from how saturation vapor pressure is calculated.

The sensitivity of  $WBGT_{Liljegen}$  and  $WBGT_{Brimicombe}$  is highly similar for solar radiation and wind speed and can be suggested to provide further evidence that Equations 2 and 6 are comparable. This is despite the potential discrepancies that were suggested in Section 2.3. This should be explored further to inform more about the inter-dependencies of the different types of radiation. Further we find that  $WBGT$  does not have a dynamical response to wind similar to previous findings and this can be suggested to be a limitation of the heat stress index (Foster et al., 2022).

### 3.5. $WBGT_{Brimicombe}$ Observations Comparisons

$WBGT_{Brimicombe}$  for reanalysis data performs robustly in comparison to  $WBGT_{Liljegen}$  it also performs accurately compared to  $WBGT_{Brimicombe}$  observed (Figure 6).  $WBGT_{Brimicombe}$  has  $R^2$  values between its ERA5 values and observation values of between 0.56 and 1 (Figures 6b–6e). It performs better for the TAT station (Tateno) situated in Japan, where  $WBGT$  values are higher than the NYA (Nya Långnäs) station situated in the Arctic circle in Svalbard overall. MAE values range from 0.97°C to 5.06°C (Figures 6b–6e). The  $R^2$  and error values are comparable with those seen between observed MRT and ERA5 MRT in Di Napoli et al. (2020).

In addition, when evaluating the Stull method in comparison to the Davies-Jones method to calculate WBT for March 2013 in the observed data small differences are observed (Table 2). The biggest MAE value is 1.43°C in WBT for NYA decreasing to 1 C in  $WBGT$ . The least significant  $R^2$  value is 0.61 for WBT for TAT. It therefore can be suggested that using Stull in comparison to Davies-Jones makes no substantial difference in the resulting  $WBGT$ .

## 4. Discussion

### 4.1. Why Another $WBGT$ Approximation?

We demonstrate that  $WBGT_{Brimicombe}$  is a useful approximation of  $WBGT$ . As discussed in Section 2.4 and supported by the results in Section 3.4,  $WBGT_{Brimicombe}$  is a beneficial method to use in the place of  $WBGT_{Liljegen}$  for gridded data sets and numerical weather prediction services. Comparisons between  $WBGT_{Brimicombe}$  and  $WBGT_{Liljegen}$  show only small differences (a difference of 1 heat stress category and a MAE of between 0.76°C and 1.13°C) across the case studies considered.  $WBGT_{Brimicombe}$  reanalysis has at most an MAE value of 5°C in comparison to it being observed (Figure 6).  $WBGT_{Brimicombe}$  performs with the least accuracy in cold climates such as Greenland and at higher altitudes such as the Tibetan Plateau, regions that are not highly populated and are cold which is outside the scope of a heat stress index (Figure 3). As such, it has been shown with confidence that  $WBGT_{Brimicombe}$  can be considered an accurate approximation of  $WBGT$  (Figures 1–6).

There are many approaches to calculating the  $WBGT$  and these derive from the fact that measurements from globe and wet bulb thermometers are not widely available (Dally et al., 2018; Lemke & Kjellstrom, 2012; Lima et al., 2021; Orlov et al., 2020; Yengoh & Ardö, 2020). Unless measurements come from these instruments and provide all the input parameters required in Equation 1, all approaches to calculate the  $WBGT$  are approximations, which are wide ranging in accuracy, a wide scale observation study, in terms of both weather and physiological observations would therefore be beneficial. This research, however, clearly demonstrates that the approximation by the American college of sports medicine,  $WBGT_{ACSM87}$ , is not an accurate indication of  $WBGT$  and recommends that it is not used for a like-for-like approximation. This finding is in agreement with current literature on the topic (Chen et al., 2019; Grundstein & Cooper, 2018; Kong & Huber, 2021; Lemke & Kjellstrom, 2012; Lima et al., 2021; Orlov et al., 2020; Yengoh & Ardö, 2020).

Previous research has suggested that the approximation by Davies-Jones (2008) is a more accurate approximation of natural WBT than the approximation by Stull (Buzan et al., 2015). However, the results presented here demonstrate the accuracy of the  $WBGT_{Brimicombe}$  results and the similar sensitivity of this approximation using Stull (2011) in comparison to  $WBGT_{Liljegen}$  and observed calculations of  $WBGT_{Brimicombe}$ . Further, for observation data it has been shown by this study that there is no more than a 1°C MAE between a  $WBGT$  output using Davies-Jones (2008) in comparison to Stull (2011). In addition, and of particularly practical relevance, the approximation by Stull (2011) is not iterative and therefore easier to use and more readily scalable than the Davies-Jones approximation.  $WBGT_{Brimicombe}$  was developed for gridded data sets from numerical weather

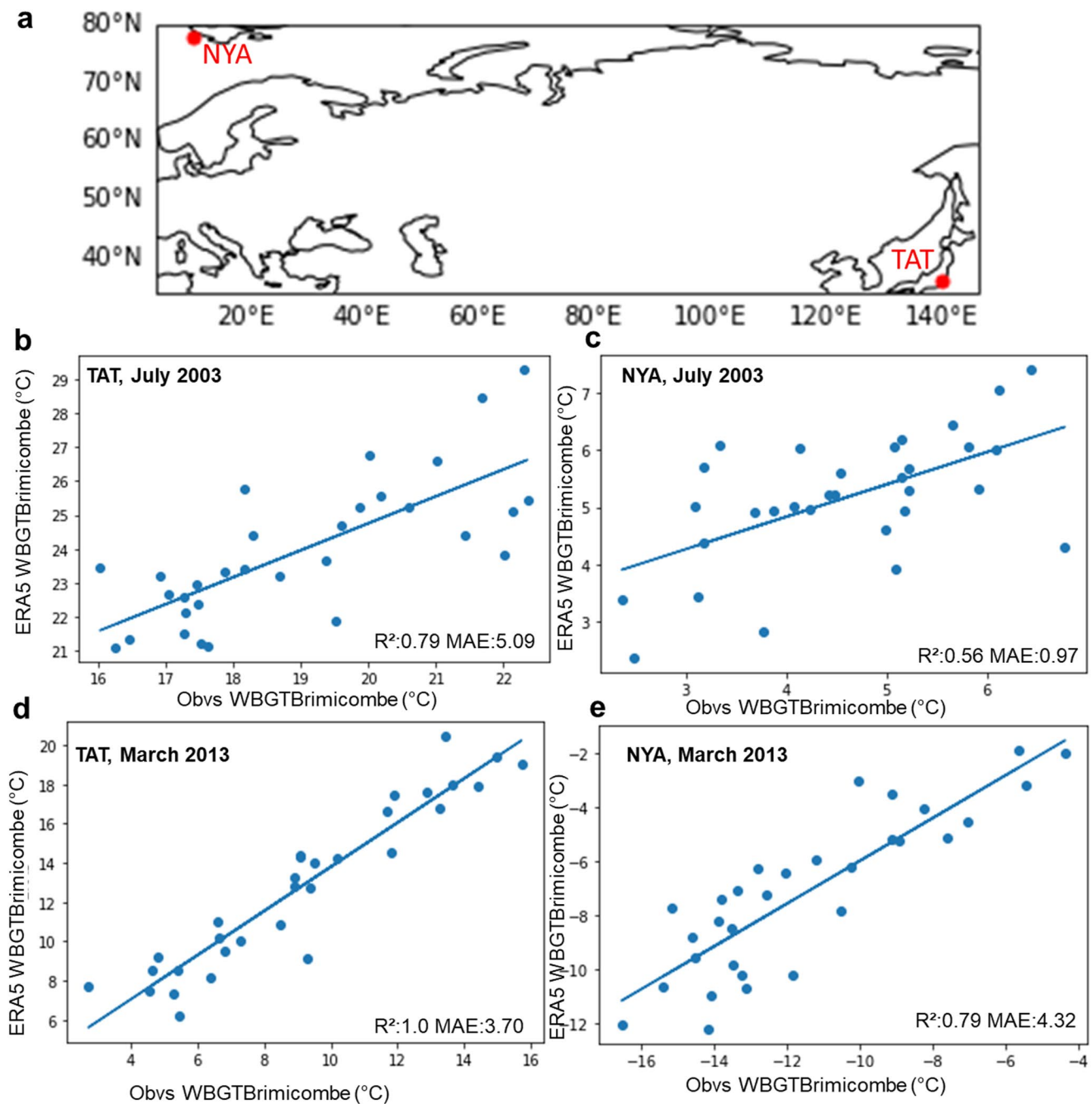


**Figure 6.** (a) The location of the observation stations NYA and TAT from the Baseline Surface Radiation Network data set to calculate observed Wet Bulb Globe Temperature using the method in thermofeel termed  $WBGT_{Brimicombe}$ . (b–e) The linear relationship,  $R^2$  and mean absolute error values for (b) TAT Daily Max July 2003, (c) NYA Daily Max July 2003, (d) TAT Daily Max March 2013, and (e) NYA Daily Max March 2013.

prediction data sets and is as accurate as  $WBGT_{Liljegren}$  whilst removing the need for complicated iterative convergence methods that can practically take a long time to run and are not readily designed for gridded data. Given all of this evidence it is unnecessary to assess Davies-Jones further by this study.

#### 4.2. How Useful Are Set Thresholds for WBGT?

$WBGT_{ACSM87}$  was found to be significantly lower than  $WBGT_{Liljegren}$  for heat stress categories and overall is not an accurate indication of WBGT heat stress risk (as per Kong and Huber (2021)). This could be of particular



**Table 2**  
*The Mean Absolute Error and  $R^2$  Values Between Stull Wet Bulb Temperature (WBT) and Davies-Jones WBT and When They Are Subsequently Used to Calculate Wet Bulb Globe Temperature for Two Sets of Observations Taken During March 2013*

| Station  | Wet bulb temperature |       | Wet bulb globe temperature |       |
|----------|----------------------|-------|----------------------------|-------|
|          | Mean absolute error  | $R^2$ | Mean absolute error        | $R^2$ |
| TAT 2013 | 0.808                | 0.611 | 0.56                       | 0.81  |
| NYA 2013 | 1.431                | 0.898 | 1                          | 0.94  |

disadvantage to the health sector where thresholds are often used to identify life-threatening conditions or to recommend heat-suitable workloads (Budd, 2008; Chen et al., 2019; Jendritzky et al., 2012; Zare et al., 2019).

In this study, it is demonstrated that  $WBGT_{Brimicombe}$  can use the same thresholds to indicate heat stress as  $WBGT_{Liljegen}$  with these being meaningful values for hazard preparedness. The deliberate decision is taken to use heat stress categories for WBGT as set out by Jacklitsch et al. (2016), where the highest value of 33°C has been shown to be a critical level for heat stress illnesses and to correlate with an increase in hospital admissions and mortality (Cheng et al., 2019). Many studies assessing heat stress and extreme heat are now making use of percentiles compared to a climate (Guigma et al., 2020; Heo et al., 2019) or a standard deviation compared to average conditions (Harrington & Otto, 2020). Whilst we acknowledge that heat

indexes and their studies, as the present one, often still do not take into account acclimatization and that 26°C will not be experienced the same by someone in the UK in comparison to Australia (Buzan & Huber, 2020; Nazarian & Lee, 2021), we see the categorical approach as fundamental to heat hazard preparedness. We support more research into acclimatization and how to best model this with heat stress thresholds and health outcomes in mind.

### 4.3. The Use of WBGT in Weather Forecasting

The WBGT is widely used across sectors. Our approach to the WBGT has been validated in its component parts, namely in the globe thermometer temperature and the wet bulb thermometer temperature (De Dear, 1987; Guo et al., 2018; Stull, 2011). It has been demonstrated for the first time (Section 3.4) that the  $T_g$  method of  $WBGT_{Brimicombe}$  and  $WBGT_{Liljegen}$  are comparable. Going forward this could be used to inform more about radiation. In addition, it is designed for easy integration into operational weather prediction outputs and for use with gridded data sets, with a view to forecast heat stress and heatwaves on a global scale (Brimicombe, Di Napoli et al., 2022).

The ISO status of the WBGT makes it stand out as a heat index that is worth forecasting across multiple sectors (Heo et al., 2019). It is important to forecast WBGT to inform decisions about heat stress warnings and adaptations. There are many benefits when forecasts are made openly accessible and many factors to consider (Budd, 2008; Buzan et al., 2015; Lemke & Kjellstrom, 2012). These include: the accuracy of a WBGT approximation in comparison to the ISO observed values used in Equation 1; the robustness of thresholds in indicating heat hazards and heat stress risk levels; the appropriateness of WBGT for different climates and acclimatization levels (Ahn et al., 2022; Budd, 2008; D'Ambrosio Alfano et al., 2014). These factors also hold true for other heat indices and should be carefully considered (Ahn et al., 2022; Zare et al., 2019).

## 5. Conclusion

$WBGT_{Brimicombe}$  has been demonstrated to be an accurate approximation of WBGT.  $WBGT_{Brimicombe}$  is within 1 heat stress category of  $WBGT_{Liljegen}$  across the land surface and in general has anomalies of no more than  $\pm 2^\circ\text{C}$  for the 3 heatwave case studies here chosen. In addition, it has a strong positive correlation with  $WBGT_{Liljegen}$  and low MAE. In addition, the  $T_g$  method for  $WBGT_{Brimicombe}$  can be suggested to be equivalent to that of  $WBGT_{Liljegen}$  enhancing understanding of the relationship of different forms of radiation. Further,  $WBGT_{Brimicombe}$  has a strong linear relationship between its observed and reanalysis data and at most an MAE of 5°C.

$WBGT_{ACSM87}$  is not an accurate approximation of WBGT and should not be continued to be used.  $WBGT_{ACSM87}$  often has a three heat stress category difference to  $WBGT_{Liljegen}$  and it widely has anomalies of  $\pm 4^\circ\text{C}$  for the three heatwave case studies chosen. Although  $WBGT_{ACSM87}$  has a strong positive correlation with  $WBGT_{Liljegen}$ , it shows high MAE values.

It is hoped that by integrating  $WBGT_{Brimicombe}$  into reanalysis, climate models and forecasts, that this information would be made openly accessibly and incorporated into sectors heat warning and adaptations, providing improvements to early warning systems and adaptation policy. Finally,  $WBGT_{Brimicombe}$  is a worthy heat stress index candidate for a global forecasting early warning system and would not only be beneficial to a range of sectors but also has the real potential to save lives.



## Nomenclature

|                         |   |
|-------------------------|---|
| $\cos \theta$           | Cosine of the solar zenith angle ( $^{\circ}$ )   |
| $h_{cg}$                | mean convection coefficient ( $\text{W}/\text{m}^2\text{K}$ )   |
| $A_h$                   | the convective heat transfer coefficient ( $\text{W}/\text{m}^2\text{K}$ )                                    |
| $T_a$                   | 2 m Temperature/Dry Bulb Temperature in K or $^{\circ}\text{C}$ as described                                  |
| $T_g$                   | Globe Temperature in K or $^{\circ}\text{C}$ as described   |
| $T_w$                   | Wet Bulb Temperature in K or $^{\circ}\text{C}$ as described  |
| $e_a$                   | Saturation vapor pressure of the air (kpa)  |
| $e_w$                   | Saturation vapor pressure of the wick (kpa)   |
| $\alpha_g$              | albedo of the globe (0.05)  |
| $\alpha_{\text{sf}c}$   | albedo of the surface (0.45)  |
| $\epsilon_a$            | the emissivity of the air ( $\text{W}/\text{m}^2$ )   |
| $\epsilon_g$            | the emissivity of the globe (0.95)  |
| $\Delta F_{\text{net}}$ | the net radiant heat flux ( $\text{W}/\text{m}^2\text{K}$ )   |
| $D$                     | Globe Diameter 0.15 m   |
| $\text{dsrp}$           | downward solar radiation proportion ( $\text{W}/\text{m}^2$ )   |
| $h$                     | mean convection coefficient ( $\text{W}/\text{m}^2\text{K}$ )   |
| $\text{ssrd}$           | Solar Surface Radiation downwards ( $\text{W}/\text{m}^2$ )   |
| $T_{\text{MRT}}$        | Mean Radiant Temperature in K or $^{\circ}\text{C}$ as described  |
| $v_a$                   | 10 m wind speed m/s   |
| $\epsilon$              | Emissivity 0.98 that of a clothed body (Bedford & Warner, 1934; De Dear, 1987)                                |
| $\text{Nu}$             | Nusselt Number is the ratio of convective to conductive heat transfer (dimensionless)                         |
| $P$                     | Surface Pressure (kpa)  |
| $\text{Pr}$             | Prandtl Number is the ratio of momentum diffusivity to thermal diffusivity (dimensionless)                    |
| $R$                     | Relative Humidity (%)   |
| $\text{Sh}$             | Sherwood Number a mass transfer operation (dimensionless)   |
| $\text{Sc}$             | Schmidt Number is the ratio of the kinematic viscosity to the molecular diffusion coefficient (dimensionless) |
| $a$                     | is a constant of the value 0.56   |
| $e$                     | Saturation Water Vapor Pressure Hpa (hPa)   |
| $\sigma$                | the Stefan-Boltzmann constant (dimensionless)   |

## Conflict of Interest

The authors declare no conflicts of interest relevant to this study.

## Data Availability Statement

ERA5 is freely accessible from Hersbach et al. (2020).  $\text{WBGT}_{\text{Brimicombe}}$  and  $\text{WBGT}_{\text{ACSM87}}$  can be calculated using *thermofeel* (Brimicombe et al., 2021, 2022) and  $\text{WBGT}_{\text{Liljegren}}$  is available on request from Kong and Huber (2021).

## References

- Ahn, Y., Uejio, C. K., Rennie, J., & Schmit, L. (2022). Verifying experimental wet bulb globe temperature hindcasts across the United States. *GeoHealth*, 6(4), e2021GH000527. <https://doi.org/10.1029/2021GH000527>
- American college of sports medicine. (1987). American college of sports medicine position stand on: The prevention of thermal injuries during distance running. *Medicine & Science in Sports & Exercise*, 19(5).
- Bedford, T., & Warner, C. G. (1934). The globe thermometer in studies of heating and ventilation. *Journal of Hygiene*, 34(4), 458–473. <https://doi.org/10.1017/S0022172400043242>
- Brimicombe, C., Di Napoli, Claudia, Q., Tiago, Pappenberger, F., Cornforth, R., & Cloke, H. L. (2021). *thermofeel*. <https://doi.org/10.21957/mp6v-fd16>
- Brimicombe, C., Di Napoli, C., Quintino, T., Pappenberger, F., Cornforth, R., & Cloke, H. L. (2022). *thermofeel*: A python thermal comfort indices library. *Software X*, 18, 101005. <https://doi.org/10.1016/J.SOFTX.2022.101005>
- Brimicombe, C., Quintino, T., Smart, S., Di Napoli, C., Hogan, R., Cloke, H. L., & Pappenberger, F. (2022). Calculating the cosine of the solar zenith angle for thermal comfort indices. Retrieved from <https://www.ecmwf.int/en/elibrary/20336-calculating-cosine-solar-zenith-angle-thermal-comfort-indices>

## Acknowledgments

This research was part funded by the European Union's Horizon 2020 Research and Innovation programme under Grant Agreement 824115. It was also part funded by NERC through the SCENARIO DTP. Claudia Di Napoli is supported by a Wellcome Trust Grant (209734/Z/17/Z). We would like to thank Qinqin Kong for providing the  $\text{WBGT}_{\text{Liljegren}}$  data set and Jonathan Buzan for initial discussions about analysis and Cascade Tuholske for discussions about observed  $\text{WBGT}$  data.

- Brunamonti, S., Füzér, L., Jorge, T., Poltera, Y., Oelsner, P., Meier, S., et al. (2019). Water vapor in the Asian summer monsoon anticyclone: Comparison of balloon-borne measurements and ECMWF data. *Journal of Geophysical Research: Atmospheres*, *124*(13), 7053–7068. <https://doi.org/10.1029/2018JD030000>
- Budd, G. M. (2008). Wet-bulb globe temperature (WBGT)-its history and its limitations. *Journal of Science and Medicine in Sport*, *11*(1), 20–32. <https://doi.org/10.1016/j.jsams.2007.07.003>
- Buzan, J. R., & Huber, M. (2020). Moist heat stress on a hotter Earth. *Annual Review of Earth and Planetary Sciences*, *48*(1), 623–655. <https://doi.org/10.1146/annurev-earth-053018-060100>
- Buzan, J. R., Oleson, K., & Huber, M. (2015). Implementation and comparison of a suite of heat stress metrics within the Community Land Model version 4.5. *Geoscientific Model Development*, *8*(2), 151–170. <https://doi.org/10.5194/GMD-8-151-2015>
- Casanueva, A. (2017). HEATSTRESS R package. <https://doi.org/10.5281/zenodo.3264929>
- Chen, X., Li, N., Liu, J., Zhang, Z., & Liu, Y. (2019). Global heat wave hazard considering humidity effects during the 21st century. *International Journal of Environmental Research and Public Health*, *16*(9), 1513. <https://doi.org/10.3390/ijerph16091513>
- Cheng, Y. T., Lung, S. C. C., & Hwang, J. S. (2019). New approach to identifying proper thresholds for a heat warning system using health risk increments. *Environmental Research*, *170*, 282–292. <https://doi.org/10.1016/j.envres.2018.12.059>
- CRED. (2020). EM-DAT | the international disasters database. Retrieved from <https://www.emdat.be/>
- Dally, M., Butler-Dawson, J., Krisher, L., Monaghan, A., Weitzenkamp, D., Sorensen, C., et al. (2018). The impact of heat and impaired kidney function on productivity of Guatemalan sugarcane workers. *PLoS One*, *13*(10), e0205181. <https://doi.org/10.1371/JOURNAL.PONE.0205181>
- D'Ambrosio Alfano, F. R., Malchaire, J., Palella, B. I., & Riccio, G. (2014). WBGT index revisited after 60 years of use. *Annals of Occupational Hygiene*, *58*(8), 955–970. <https://doi.org/10.1093/annhyg/meu050>
- Davies-Jones, R. (2008). An efficient and accurate method for computing the wet-bulb temperature along pseudoadiabats. *Monthly Weather Review*, *136*(7), 2764–2785. <https://doi.org/10.1175/2007MWR2224.1>
- De Dear, R. (1987). Ping-pong globe thermometers for mean radiant temperatures. *Heating and Ventilation Engineer and Journal of Air Conditioning*, *60*, 10–11. Retrieved from <https://ci.nii.ac.jp/naid/10030966825>
- Di Napoli, C., Barnard, C., Prudhomme, C., Cloke, H. L., & Pappenberger, F. (2021). ERA5-HEAT: A global gridded historical dataset of human thermal comfort indices from climate reanalysis. *Geoscience Data Journal*, *8*(1), 2–10. <https://doi.org/10.1002/gdj3.102>
- Di Napoli, C., Hogan, R. J., & Pappenberger, F. (2020). Mean radiant temperature from global-scale numerical weather prediction models. *International Journal of Biometeorology*, *64*(7), 1233–1245. <https://doi.org/10.1007/s00484-020-01900-5>
- Driemel, A., Augustine, J., Behrens, K., Colle, S., Cox, C., Cuevas-Agulló, E., et al. (2018). Baseline surface radiation network (BSRN): Structure and data description (1992–2017). *Earth System Science Data*, *10*(3), 1491–1501. <https://doi.org/10.5194/essd-10-1491-2018>
- Foster, J., Smallcombe, J. W., Hodder, S., Jay, O., Flouris, A. D., & Havenith, G. (2022). Quantifying the impact of heat on human physical work capacity; part II: The observed interaction of air velocity with temperature, humidity, sweat rate, and clothing is not captured by most heat stress indices. *International Journal of Biometeorology*, *66*(3), 507–520. <https://doi.org/10.1007/S00484-021-02212-Y/FIGURES/6>
- Freychet, N., Tett, S. F. B., Yan, Z., & Li, Z. (2020). Underestimated change of wet-bulb temperatures over east and South China. *Geophysical Research Letters*, *47*(3), e2019GL086140. <https://doi.org/10.1029/2019GL086140>
- Grundstein, A., & Cooper, E. (2018). Assessment of the Australian Bureau of Meteorology wet bulb globe temperature model using weather station data. *International Journal of Biometeorology*, *62*(12), 2205–2213. <https://doi.org/10.1007/S00484-018-1624-1>
- Guigma, K. H., Todd, M., & Wang, Y. (2020). Characteristics and thermodynamics of Sahelian heatwaves analysed using various thermal indices. *Climate Dynamics*, *1*(11–12), 3151–3175. <https://doi.org/10.1007/s00382-020-05438-5>
- Guo, H., Teitelbaum, E., Houchois, N., Bozlar, M., & Meggers, F. (2018). Revisiting the use of globe thermometers to estimate radiant temperature in studies of heating and ventilation. *Energy and Buildings*, *180*, 83–94. <https://doi.org/10.1016/j.enbuild.2018.08.029>
- Hardy, B. (1998). ITS-90 formulations for vapor pressure, frostpoint temperature, dewpoint temperature, and enhancement factors in the range –100 to +100 C. In *The proceedings of the third international symposium on humidity & moisture*, (pp. 1–8).
- Harrington, L. J., & Otto, F. E. L. (2020). Reconciling theory with the reality of African heatwaves. *Nature Climate Change*, *1*(9), 796–798. <https://doi.org/10.1038/s41558-020-0851-8>
- Heo, S., Bell, M. L., & Lee, J. T. (2019). Comparison of health risks by heat wave definition: Applicability of wet-bulb globe temperature for heat wave criteria. *Environmental Research*, *168*, 158–170. <https://doi.org/10.1016/j.envres.2018.09.032>
- Hersbach, H., Bell, B., Berrisford, P., Hirahara, S., Horányi, A., Muñoz-Sabater, J., et al. (2020). The ERA5 global reanalysis. *Quarterly Journal of the Royal Meteorological Society*, *146*(730), 1999–2049. <https://doi.org/10.1002/qj.3803>
- Hogan, R. J., & Hirahara, S. (2016). Effect of solar zenith angle specification in models on mean shortwave fluxes and stratospheric temperatures. *Geophysical Research Letters*, *43*(1), 482–488. <https://doi.org/10.1002/2015GL066868>
- Int Org Standard. (2017). *Ergonomics of the thermal environment - Assessment of heat stress using the WBGT (wet bulb globe temperature) index - ISO 7243:2017*. International Standards Organisation.
- Ioannou, L. G., Tsoutsoubi, L., Mantzios, K., Vliora, M., Nintou, E., Pii, J. F., et al. (2022). Indicators to assess physiological heat strain – Part 3: Multi-country field evaluation and consensus recommendations. *Temperature*, *9*(3), 274–291. <https://doi.org/10.1080/23328940.2022.2044739>
- Jacklitsch, B., Williams, J., Musolin, K., Coca, A., Kim, J.-H., & Turner, N. (2016). Criteria for a recommended standard: Occupational exposure to heat and hot environments.
- Jendritzky, G., de Dear, R., & Havenith, G. (2012). UTCI-Why another thermal index? *International Journal of Biometeorology*, *56*(3), 421–428. <https://doi.org/10.1007/s00484-011-0513-7>
- Kjellstrom, T., Holmer, I., & Lemke, B. (2009). Workplace heat stress, health and productivity-an increasing challenge for low and middle-income countries during climate change. *Global Health Action*, *2*(1), 2047. <https://doi.org/10.3402/gha.v2i0.2047>
- Kong, Q., & Huber, M. (2021). Explicit calculations of wet bulb globe temperature compared with approximations and why it matters for labor productivity. <https://doi.org/10.1002/ESSOAR.10507637.1>
- Kong, Q., & Huber, M. (2022). Explicit calculations of wet-bulb globe temperature compared with approximations and why it matters for labor productivity. *Earth's Future*, *10*(3), e2021EF002334. <https://doi.org/10.1029/2021EF002334>
- Lemke, B., & Kjellstrom, T. (2012). Calculating workplace WBGT from meteorological data: A tool for climate change assessment. *Industrial Health*, *50*(4), 267–278. <https://doi.org/10.2486/indhealth.MS1352>
- Liljegren, J. C., Carhart, R. A., Lawday, P., Tschopp, S., & Sharp, R. (2008). Modeling the wet bulb globe temperature using standard meteorological measurements. *Journal of Occupational and Environmental Hygiene*, *5*(10), 645–655. <https://doi.org/10.1080/15459620802310770>
- Lima, C. Z. D., Buzan, J. R., Moore, F. C., Baldos, U. L. C., Huber, M., & Hertel, T. W. (2021). Heat stress on agricultural workers exacerbates crop impacts of climate change. *Environmental Research Letters*, *16*(4), 044020. <https://doi.org/10.1088/1748-9326/ABEB9F>
- Lucas, R. A. I., Epstein, Y., & Kjellstrom, T. (2014). Excessive occupational heat exposure: A significant ergonomic challenge and health risk for current and future workers. *Extreme Physiology & Medicine*, *3*(1), 14. <https://doi.org/10.1186/2046-7648-3-14>

- McGregor, G. R., & Vanos, J. K. (2018). Heat: A primer for public health researchers. *Public Health*, *161*, 138–146. <https://doi.org/10.1016/j.puhe.2017.11.005>
- Minard, D. (1961). Prevention of heat casualties in Marine Corps recruits. Period of 1955–60, with comparative incidence rates and climatic heat stresses in other training categories. *Military Medicine*, *126*(4), 261–272. <https://doi.org/10.1093/milmed/126.4.261>
- Nazarian, N., & Lee, J. K. W. (2021). Personal assessment of urban heat exposure: A systematic review. *Environmental Research Letters*, *16*(3), 033005. <https://doi.org/10.1088/1748-9326/abd350>
- Orlov, A., Sillmann, J., Aunan, K., Kjellstrom, T., & Aaheim, A. (2020). Economic costs of heat-induced reductions in worker productivity due to global warming. *Global Environmental Change*, *63*, 102087. <https://doi.org/10.1016/j.gloenvcha.2020.102087>
- Parsons, K. (2006). Heat stress standard ISO 7243 and its global application. *Industrial Health*, *44*(3), 368–379. <https://doi.org/10.2486/indhea.lth.44.368>
- Racinais, S., Alonso, J. M., Coutts, A. J., Flouris, A. D., Girard, O., González-Alonso, J., et al. (2015). Consensus recommendations on training and competing in the heat. *Scandinavian Journal of Medicine & Science in Sports*, *25*, 6–19. <https://doi.org/10.1007/s40279-015-0343-6>
- Raymond, C., Singh, D., & Horton, R. M. (2017). Spatiotemporal patterns and synoptics of extreme wet-bulb temperature in the contiguous United States. *Journal of Geophysical Research: Atmospheres*, *122*(24), 13108–13124. <https://doi.org/10.1002/2017JD027140>
- Senyunzi, R. C., Oruru, B., D'ujanga, F. M., Realini, E., Barindelli, S., Tagliaferro, G., et al. (2020). Performance of ERA5 data in retrieving precipitable water vapour over east African tropical region. *Advances in Space Research*, *65*(8), 1877–1893. <https://doi.org/10.1016/j.asr.2020.02.003>
- Spangler, K. R., Liang, S., & Wellenius, G. A. (2022). Wet-bulb globe temperature, universal thermal climate index, and other heat metrics for US counties, 2000–2020. *Scientific Data*, *9*(1), 326. <https://doi.org/10.1038/s41597-022-01405-3>
- Stull, R. (2011). Wet-bulb temperature from relative humidity and air temperature. *Journal of Applied Meteorology and Climatology*, *50*(11), 2267–2269. <https://doi.org/10.1175/JAMC-D-11-0143.1>
- Thorsson, S., Lindberg, F., Eliasson, I., & Holmer, B. (2007). Different methods for estimating the mean radiant temperature in an outdoor urban setting. *International Journal of Climatology*, *27*(14), 1983–1993. <https://doi.org/10.1002/JOC.1537>
- Vanos, J. K., Rykaczewski, K., Middel, A., Vecellio, D. J., Brown, R. D., & Gillespie, T. J. (2021). Improved methods for estimating mean radiant temperature in hot and sunny outdoor settings. *International Journal of Biometeorology*, *65*(6), 967–983. <https://doi.org/10.1007/S00484-021-02131-Y>
- Yengoh, G. T., & Ardö, J. (2020). Climate change and the future heat stress challenges among smallholder farmers in east Africa. *Atmosphere*, *11*(7), 753. <https://doi.org/10.3390/ATMOS11070753>
- Zare, S., Shirvan, H. E., Hemmatjo, R., Nadri, F., Jahani, Y., Jamshidzadeh, K., & Paydar, P. (2019). A comparison of the correlation between heat stress indices (UTCI, WBGT, WBGT, TSI) and physiological parameters of workers in Iran. *Weather and Climate Extremes*, *26*, 100213. <https://doi.org/10.1016/j.wace.2019.100213>